

## ATIC flight data processing

H. S. Ahn for the ATIC collaboration

Inst. for Phys. Sci. and Tech., University of Maryland, College Park, MD 20742, USA

### Abstract.

The first flight of the Advanced Thin Ionization Calorimeter (ATIC) experiment from McMurdo, Antarctica lasted for 16 days, starting on December 28, 2000. The ATIC instrument consists of a fully active 320-crystal, 960-channel Bismuth Germanate (BGO) calorimeter, 202 scintillator strips (808 channels) in 3 hodoscopes, interleaved with graphite target layers, and a 4480-pixel silicon matrix charge detector. We have developed an object-oriented data processing package based on ROOT. In this paper, we describe the data processing scheme used in handling the accumulated 45 GB of flight data. We discuss calibration issues, particularly the time-dependence of housekeeping information.

### 1 Introduction

The Advanced Thin Ionization Calorimeter (ATIC) investigation is designed to measure the composition and energy spectra of cosmic rays over the energy range from 10 GeV to 100 TeV in a series of several (3 - 4) balloon flights. Its first long duration (16 days) balloon test flight from McMurdo, Antarctica lasted from December 28, 2000 to January 13, 2001. It collected about  $3 \times 10^7$  events which amounted to 45 GB of data. The flight data has been studied since, and various preliminary results are provided by companion papers at this conference (Adams et al., 2001a,b; Fazely and Gunasingha et al., 2001; Isbert et al., 2001; Seo et al., 2001; Wefel et al., 2001; Zatsepin et al., 2001).

### 2 ATIC Instrument

The ATIC instrument (schematic shown in Wefel et al., 2001) has three major components with a total of 6248 channels: 1) a Si matrix ( $80 \times 56$ ) for charge determination, comprised of 4480 pixels (4480 channels), 2) a trapezoid-shaped graphite

target to induce nuclear interactions, interleaved with a set of plastic scintillator hodoscopes (S1, S2, S3 from the top down) with a 2-range PMT readout on each side (808 channels), and 3) an electromagnetic calorimeter, to measure cascade energy from primary interactions, that is comprised of eight layers of 40 BGO crystals each, with a 3-range PMT readout (960 channels).

### 3 Data Processing

#### 3.1 ATIC Data Processing System

The ATIC Data Processing System (ADPS) based on ROOT (Brun and Rademakers, 1997) has been developed and its ability has been demonstrated in on-line monitoring during the flight and in off-line calibration and data processing.

ROOT, developed at CERN for high energy experiments, provides a powerful object-oriented data analysis framework and presentation tool. Written in C++, ROOT can interpret C/C++ scripts and incorporates user-defined classes and methods optimized for specific experiments. Large scripts can be compiled into shared libraries and dynamically integrated into the ROOT environment. ROOT also provides various tools for creating multi-dimensional histograms and ntuples, fitting, minimization, on-screen editing, etc.

For ATIC data processing, the ADPS incorporates various classes and methods: 1) 'data-reader' which generates Level 0 output by reading, unpacking and sorting raw data, 2) 'calibrator' which generates Level 1 output by converting ADC counts to energy units, 3) 'shower-handler' which generates Level 2 output by calculating event parameters such as total energy deposit, layer energy deposit, trajectory, charge, etc., 4) 'event-display' which provides graphic information utilizing various functions such as zoom, 3-D rotations, etc.

#### 3.2 Level 0

The ATIC Flight Data System recorded the data in binary format and produced 633 time-ordered raw datasets. These

datasets include a series of event records of various types (Event, Calibrate, Housekeeping, etc.) and subtypes, each with its own header, subheader and data records. The datasets can be sorted according to the types and subtypes into separate Level 0 data files which can be studied for various purposes: 1) 'Event' includes all the channels' sparsified pulse height amplitudes and electronic addresses which are mapped to physical pixels, strips and crystals with their location, 2) 'Calibrate' includes pedestal, LED flasher and charge-pulsers events which can be used to generate time-dependent calibration functions, 3) 'Housekeeping' includes information on physical environment (temperature, pressure, position), power system status, etc.

Typical time dependences of 'Housekeeping' (temperature) and 'Calibrate' (BGO pedestal) measurements are shown in Figs. 1 and 2, respectively.

### 3.3 Calibration

The low-range responses for BGO crystals, scintillator strips, and Si pixels were calibrated using cosmic-ray muons accumulated before the flight. After pedestal subtraction for each low-range channel, cosmic-ray muon distributions were made and fitted with combinations of Gaussian plus exponential functions to locate the most probable value. The exponential term was added to account for the corner-clipping effect. A typical example of this procedure is shown in Fig. 3. Comparing these values among crystals (also strips or pixels) allowed the relative inter-crystal (strip or pixel) calibration. Absolute calibration was provided by comparing with simulation results using the GEANT 3.21 package (Brun et al., 1984). Muons were generated according to known cosmic-ray muon energy and angular distributions and filtered through simple conditions similar to the ATIC pre-trigger (with requirements only on hodoscope signals). The resulting values of 25.9 MeV, 1.89 MeV and 0.143 MeV for BGO crystal, scintillator strip and Si pixel, respectively, were used to generate low-range calibration constants.

The higher-range responses were calibrated using cosmic ray showers accumulated while ATIC remained within line-of-sight (LOS). Due to poor statistics of very high energy cosmic rays, LED data were also used to calibrate the highest-range responses for BGO crystals. Two dimensional distributions were made for two different ranges for one crystal (or strip) and fitted with a linear function to estimate the slope, which was then used to calculate higher-range calibration constants. A typical example of this procedure is shown in Fig. 4.

### 3.4 Level 1

The raw pulse height amplitude was converted to physical energy units following several steps of gain corrections to generate Level 1 outputs.

As shown in Fig. 2, pedestal levels were not very time-dependent for BGO crystals (or scintillator strips) during the entire length of the flight, so the pedestal correction was done

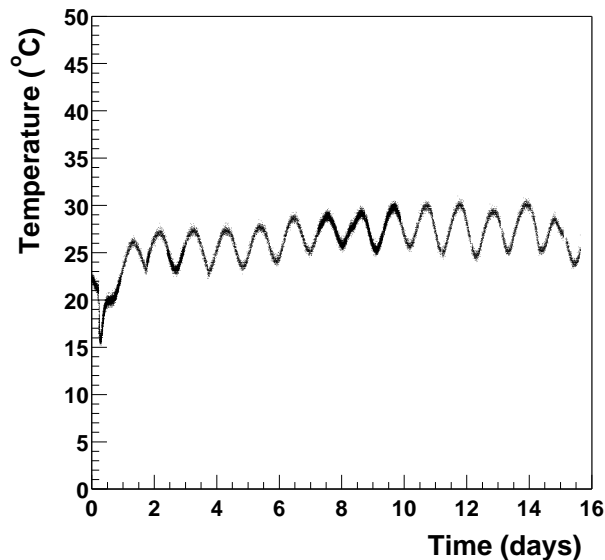


Fig. 1. An example of time dependence of a 'Housekeeping' measurement (temperature)

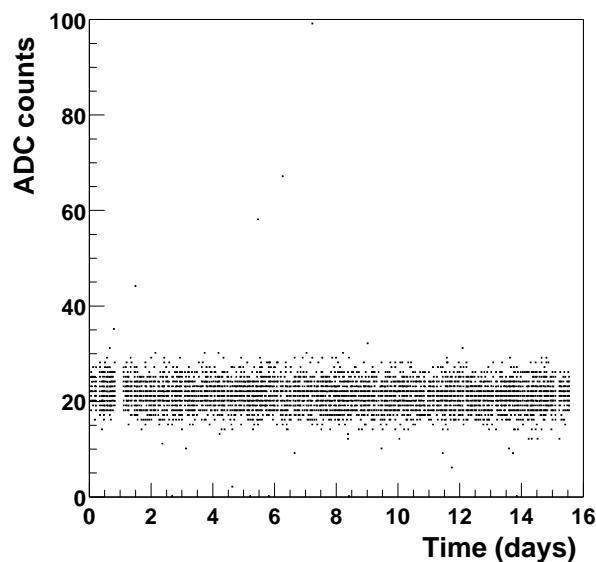
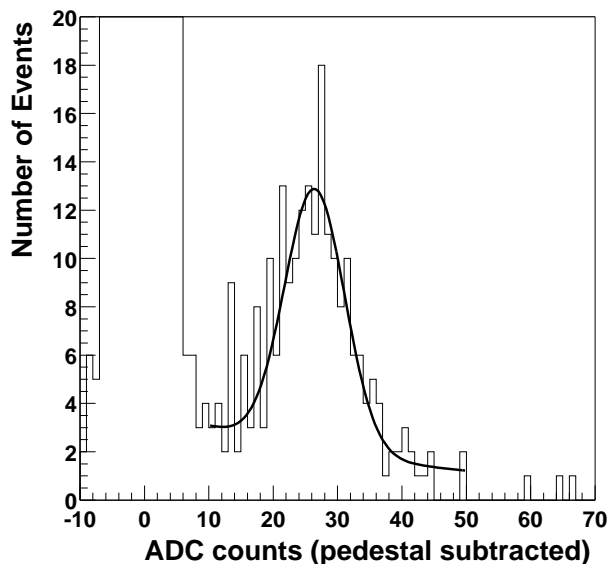
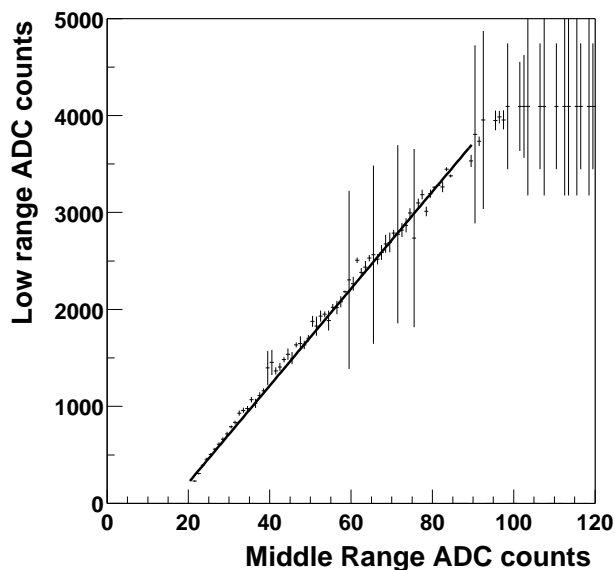


Fig. 2. An example of time dependence of a 'Calibrate' measurement (BGO pedestal)



**Fig. 3.** A typical ADC count (pedestal subtracted) distribution due to cosmic ray muons passing through a BGO crystal.



**Fig. 4.** A typical two dimensional distribution for ADC counts of 2 different ranges due to cosmic ray showers in a BGO crystal.

using a single calibration run. The Si pixels, however, showed a temperature dependence of about 20 ADC counts/ $^{\circ}$ C. For these, pedestals taken every 6 minute were applied to the 'Event's taken for the following 6 minutes to account for possible pedestal drift. The pedestal drift is estimated to be about 1.25 ADC counts per 6 minutes.

For BGO crystals (and scintillator strips), which had a 3-(2-) range readout using dynode pick-offs to cover the required dynamic range, the lowest non-saturating range was chosen and gain-corrected. For scintillator strips which had PMT readouts on each end, the two PMT signals were averaged geometrically (square-root of the product of the two signal levels) to cancel out attenuation effects.

### 3.5 Level 2

Event selection and reconstruction algorithms were used to calculate event parameters (e.g. energy deposit, trajectory, charge, etc.) which characterized each event, generating Level 2 output for science analysis. The total energy deposit is the energy sum over all 320 BGO crystals, which will be used to get the final energy spectra by deconvolution. The eight layer-energy deposits are the energy sums over 40 BGO crystals in a layer, which can be used to reject late-interacting particles, etc.

A tracking algorithm was developed to reconstruct the particle trajectories. The energy deposit centroid is calculated in each BGO layer, providing up to 4 cascade axis coordinates each for x and for y. Fitting with a straight line through the four coordinates, the shower axis is extrapolated to the Si matrix and the entrance particle position is calculated (x and y, separately). The trajectory resolution can be improved by adding information from the scintillator hodoscopes. In this case, hodoscope layers with a significant amount of energy are assumed to be below the first interaction and are treated similar to the BGO layers. The reconstructed trajectory is utilized to help charge determination by identifying the particle's entrance position and allowing pathlength corrections in the Si matrix.

Incident particle charge is determined by examining all Si pixels within a circle of confusion of the extrapolated position, selecting the largest signal as the incident particle's signal. S1 (top hodoscope) can be used to give a supplementary charge determination using a similar algorithm.

## 4 Summary

The first ATIC flight data have been processed with preliminary understanding of the instrument to produce various levels of datasets. Analysis is still in progress and more detailed studies are in progress to improve the calibration, correct for the trigger efficiency, etc. to obtain the final spectra.

*Acknowledgements.* This work was supported by NASA grants to UMD, LSU, NRL, and SU. We thank NASA WFF, NSBF, and NSF Polar programs for the balloon flight. H. S. Ahn, the main author

of this paper, was supported by American Astronomical Society, International Travel Grant Program.

## References

- Adams, J. H., et al., Preliminary Results from the First Flight of ATIC: the Silicon Matrix, this conference, 27th ICRC, 2001a.
- Adams, J. H., et al., Preliminary Results from the First Flight of ATIC:  $Z_{\leq 8}$  Spectra, this conference, 27th ICRC, 2001b.
- Brun, R., and Rademakers, F., Nucl. Instr. Meth. A389, 81, 1997.
- Brun, R., et al., GEANT User's Guide, CERN DD/EE/84-1, 1984.
- Fazely A. R. and Gunasingha R. M., et al., The CNO Concentration in Cosmic Ray Spectrum as Measured from The Advanced Thin Ionization Calorimeter Experiment, this conference, 27th ICRC, 2001.
- Ganel, O., et al., Proc. 26th ICRC (Salt Lake City), OG 4.6.01, 1999.
- Isbert, J., et al., The ATIC Experiment: Performance of the Scintillator Hodoscope and the BGO Calorimeter, this conference, 27th ICRC, 2001.
- Seo, E. S., et al., Preliminary Results from the First Flight of ATIC, this conference, 27th ICRC, 2001.
- Seo, E. S., et al., SPIE International Symposium on Optical Science, Engineering and Instrumentation, Denver, CO, 2806, 134-144, 1996.
- Wefel, J. P., et al., The ATIC Experiment: First Flight, this conference, 27th ICRC, 2001.
- Zatsepin, V. I., et al., The First Flight of ATIC: Preliminary Results on Li, Be, B Nuclei, this conference, 27th ICRC, 2001.